Martha O'Bryan

# Compendium of Single Event Effect Results from NASA Goddard Space Flight Center


Martha V. O'Bryan[1], Kenneth A. LaBel[2], Carl M. Szabo[1], Dakai Chen[2], Michael J. Campola[2], Megan C. Casey[2], Jean Marie Lauenstein[2], Edward P. Wilcox[1], Raymond L. Ladbury[2], Stanley A. Ikpe[3], Jonathan A. Pellish, [2] and Melanie D. Berg[1]

1. AS&D, Inc.; 2. NASA GSFC; 3. NASA LaRC

National Aeronautics and Space Administration



***Abstract:*** We present the results of single event effects (SEE) testing and analysis investigating the effects of radiation on electronics. This paper is a summary of test results.


## Introduction

NASA spacecraft are subjected to a harsh space environment that includes exposure to various types of ionizing radiation. The performance of electronic devices in a space radiation environment are often limited by their susceptibility to single event effects (SEE). Ground-based testing is used to evaluate candidate spacecraft electronics to determine risk to spaceflight applications. Interpreting the results of radiation testing of complex devices is challenging. Given the rapidly changing nature of technology, radiation test data are most often application-specific and adequate understanding of the test conditions is critical.

Studies discussed herein were undertaken to establish the application-specific sensitivities of candidate spacecraft and emerging electronic devices to single-event upset (SEU), single-event latchup (SEL), single-event gate rupture (SEGR), single-event burnout (SEB), and single-event transient (SET).

For total ionizing dose (TID) and displacement damage dose (DDD) results, see a companion paper submitted to the 2016 Institute of Electrical and Electronics Engineers (IEEE) Nuclear and Space Radiation Effects Conference (NSREC) Radiation Effects Data Workshop (REDW) entitled "Compendium of Total Ionizing Dose and Displacement Damage Results from NASA Goddard Space Flight Center" by M. Campola, *et al.*

## Test Techniques and Setup

### A. Test Facilities

All tests were performed between February 2015 and February 2016. Heavy ion experiments were conducted at the Lawrence Berkeley National Laboratory (LBNL), NASA Space Radiation Laboratory (NSRL) at Brookhaven National Laboratory, and at the Texas A&M University Cyclotron (TAMU). All of these facilities provide a variety of ions over a range of energies for testing. Each device under test (DUT) was irradiated with heavy ions having linear energy transfer (LET) ranging from 0.07 to 120 MeV•cm²/mg. Fluxes ranged from $1\times10^2$ to $1\times10^5$ particles/cm²/s, depending on device sensitivity. Representative ions used are listed in Tables I, II and III. LETs in addition to the values listed were obtained by changing the angle of incidence of the ion beam with respect to the DUT, thus changing the path length of the ion through the DUT and the "effective LET" of the ion. Energies and LETs available varied slightly from one test date to another.

Proton SEE tests were performed at Northwestern Medicine Chicago Proton Center (CDH), Hampton University Proton Therapy Institute (HUPTI), Massachusetts General Francis H. Burr Proton Therapy (MGH), Scripps Proton Therapy Center (Scripps), and Tri-University Meson Facility (TRIUMF).

Laser SEE tests were performed at the pulsed laser facility at the Naval Research Laboratory (NRL). Single photon absorption method was used with the laser light having a wavelength of 590 nm resulting in a skin depth (depth at which the light intensity decreased to 1/e – or about 37% – of its intensity at the surface) of 2 µm. A nominal pulse rate of 1 kHz was utilized. Pulse width was 1 ps, beam spot size ~1.2 µm.

**Table I: LBNL Test Heavy Ions**

| Ion | Energy (MeV) | Surface LET in Si (MeV•cm²/mg) (Normal Incidence) | Range in Si (µm) |
|---|---|---|---|
| $^{18}$O | 183 | 2.2 | 226 |
| $^{22}$Ne | 216 | 3.5 | 175 |
| $^{40}$Ar | 400 | 9.7 | 130 |
| $^{51}$V | 508 | 14.6 | 113 |
| $^{63}$Cu | 660 | 21.2 | 108 |
| $^{84}$Kr | 906 | 30.2 | 113 |
| $^{107}$Ag | 1039 | 48.2 | 90 |
| $^{124}$Xe | 1233 | 58.8 | 90 |
| LBNL 10 MeV per amu tune | | | |

**Table III: NSRL Test Heavy Ions**

| Ion | Energy (MeV) | Surface LET in Si (MeV•cm²/mg) (Normal Incidence) | Range in Si (µm) |
|---|---|---|---|
| $^{197}$Au | 32505 | 24.7 | 3700 |

**Table II: TAMU Test Heavy Ions**

| Ion | Energy (MeV) | Surface LET in Si (MeV•cm²/mg) (Normal Incidence) | Range in Si (µm) |
|---|---|---|---|
| $^{14}$N | 210 | 1.3 | 428 |
| $^{20}$Ne | 300 | 2.5 | 316 |
| $^{40}$Ar | 599 | 7.7 | 229 |
| $^{63}$Cu | 944 | 17.8 | 172 |
| $^{84}$Kr | 1259 | 25.4 | 170 |
| $^{109}$Ag | 1634 | 38.5 | 156 |
| $^{129}$Xe | 1934 | 47.3 | 156 |
| $^{197}$Au | 2954 | 80.2 | 155 |
| TAMU 15 MeV per amu tune | | | |
| $^{84}$Kr | 2081 | 19.8 | 332 |
| $^{129}$Xe | 3197 | 38.9 | 286 |
| TAMU 25 MeV per amu tune | | | |

amu = atomic mass unit

### B. Test Method

Unless otherwise noted, all tests were performed at room temperature and with nominal power supply voltages. Device qualification include SEL high-temperature, $V_{CC}$ plus worst-case and for SEU/SET high-temperature, $V_{CC}$ minus worst-case. Unless otherwise noted, SEE testing was performed in accordance with JESD57 test procedures where applicable.

**1) SEE Testing - Heavy Ion:**

Depending on the DUT and the test objectives, one or more of three SEE test approaches were typically used:

***Dynamic*** – the DUT was continually exercised while being exposed to the beam. The events and/or bit errors were counted, generally by capturing with a high-speed oscilloscope, digital input/output (DIO) device, microprocessor, FPGA, or by comparing the DUT output to an unirradiated reference device or with an expected output (Golden chip or virtual Golden chip methods). In some cases, the effects of clock speed or device operating modes were investigated. *Results of such tests should be applied with caution due to their application-specific nature.*

***Static*** – the DUT was configured prior to irradiation; data were retrieved and errors were counted after irradiation.

***Biased*** – the DUT was biased and clocked while power consumption was monitored for SEL or other destructive effects. In most SEL tests, functionality was also monitored.

DUTs were monitored for soft errors, such as SEUs, and for hard failures such as SEGR. Detailed descriptions of the types of errors observed are noted in the individual test reports on radhome.nasa.gov and nepp.nasa.gov.

SET testing was performed using high-speed oscilloscopes controlled via LabVIEW®. Individual criteria for SETs are specific to the device and application being tested.

Heavy ion SEE sensitivity experiments include measurement of the linear energy transfer threshold ($LET_{th}$) and cross section at the maximum measured LET. The $LET_{th}$ is defined as the maximum LET value at which no effect was observed at an effective fluence of $1\times10^7$ particles/cm². In the case where events are observed at the smallest LET tested, $LET_{th}$ will either be reported as less than the lowest measured LET or determined approximately as the $LET_{th}$ parameter from a Weibull fit. In the case of SEGR and SEB experiments, measurements are made of the SEGR or SEB threshold $V_{DS}$ (drain-to-source voltage) as a function of LET and ion energy at a fixed $V_{GS}$ (gate-to-source voltage).

**2) SEE Testing - Proton:**

Proton SEE tests were performed in a manner similar to heavy ion exposures. However, because protons usually cause SEE via indirect ionization of recoil particles, results are parameterized in terms of proton energy rather than LET. Because such proton-induced nuclear interactions are rare, proton tests also feature higher cumulative fluences and particle flux rates than heavy ion experiments.

**2) SEE Testing - Pulsed Laser Facility Testing:**

The DUT was mounted on an X-Y-Z stage in front of a 100x lens that produces a spot diameter of approximately 1 µm at full-width half-maximum (FWHM). The X-Y-Z stage can be moved in steps of 0.1 µm for accurate determination of SEE-sensitive regions in front of the focused beam. An illuminator, together with a charge-coupled device (CCD) camera and monitor, were used to image the area of interest thereby facilitating accurate positioning of the device in the beam. The pulse energy was varied in a continuous manner using a polarizer/half-waveplate combination and the energy was monitored by splitting off a portion of the beam and directing it at a calibrated energy meter.

## Test Results Overview

Principal investigators are listed in Table IV. Abbreviations and conventions are listed in Table V. SEE test results are summarized in Table VI. Unless otherwise noted all LETs are in MeV•cm²/mg and all cross sections are in cm²/device. All SEL tests are performed to a fluence of $1\times10^7$ particles/cm² unless otherwise noted.

**Table IV: List of Principal Investigators**

| Principal Investigator (PI) | Abbreviation |
|---|---|
| Melanie D. Berg | MB |
| Megan C. Casey | MCC |
| Michael J. Campola | MJC |
| Dakai Chen | DC |
| Raymond L. Ladbury | RLL |
| Jean-Marie Lauenstein | JML |
| Carl M. Szabo | CS |
| Jonathan A. Pellish | JP |
| Edward (Ted) P. Wilcox | TW |

**Table V: Abbreviations and Conventions**

LET = linear energy transfer (MeV•cm²/mg)
$LET_{th}$ = linear energy transfer threshold (the maximum LET value at which no effect was observed at an effective fluence of $1\times10^7$ particles/cm² – in MeV•cm²/mg)
< = SEE observed at lowest tested LET
> = no SEE observed at highest tested LET
σ = cross section (cm²/device, unless specified as cm²/bit)
$σ_{maxm}$ = cross section at maximum measured LET (cm²/device, unless specified as cm²/bit)
ADC = analog to digital converter
BiCMOS = bipolar complementary metal oxide semiconductor
BNL=Brookhaven National Laboratory Tandem Van de Graaff
CDH=Northwestern Medicine Chicago Proton Center
CMOS = complementary metal oxide semiconductor
CMRR = common-mode rejection ratio
DAC=Digital to Analog Converter
DUT = device under test
ECC = error correcting code
H = heavy ion test
HUPTI=Hampton University Proton Therapy Institute
$I_D$ = drain current
IC = integrated circuit
ID# = identification number
$I_{DS}$ = drain-source current
$I_G$ = gate current
Iout = output current
$I_R$ = reverse leakage current
L = laser test
LBNL = Lawrence Berkeley National Laboratory
LDC = lot date code
LVDS=Low-Voltage Differential Signaling
min = minimum
MGH=Mass General Francis H. Burr Proton Therapy
MOSFET = metal-oxide-semiconductor field-effect transistor
NAND = Negated AND or NOT AND
NRL = Naval Research Laboratory
PI = principal investigator
PIGS = post-irradiation gate stress
PSRR = power supply rejection ratio
REAG = radiation effects and analysis group
SBU = single-bit upset
Scripps = Scripps Proton Therapy Center
SEB = single event burnout
SEDR = single event dielectric rupture
SEE = single event effect
SEFI = single-event functional interrupt
SEGR = single event gate rupture
SEL = single event latchup
SET = single event transient
SEU = single event upset
SiC = silicon carbide
SMU = source-measure unit
TAMU = Texas A&M University Cyclotron Facility
TRIUMF=Tri-University Meson Facility
$V_{CC}$ = power supply voltage
VDMOS = vertical double diffused MOSFET
$V_{DS}$ = drain-to-source voltage
$V_{GS}$ = gate-to-source voltage
VNAND = vertical-NAND
$V_R$ = reverse bias voltage

## Table VI: Summary of SEE Test Results

| Part Number | Manufacturer | LDC or Wafer#; REAG ID# | Device Function | Technology | Particle: (Facility/Year/Month) P.I. | Test Results: LET in MeV•cm²/mg, σ in cm²/device, unless otherwise specified | Supply Voltage | Sample Size (Number Tested) |
|---|---|---|---|---|---|---|---|---|
| **Processors:** | | | | | | | | |
| Broadwell 5th Gen. Core™ i3-5005U | Intel | 15-080 | Processor | 14nm Gen 5 CMOS and FinFET | P: (MGH; TRIUMF; HUPTI; Scripps) CS; H: (TAMU15Aug, TAMU15Dec, TAMU16May) CS | Testing to evaluate Proton facilities and development of test processes. Test results available via Duncan, et al., at this year's Data Workshop. | 1.05V, 3.3 V | 10 |
| Skylake 6th Gen Core™ i5-6600K | Intel | 15-081 | Processor | 14nm Gen 6 CMOS and FinFET | P: (TRIUMF15Nov) CS | Testing to evaluate Proton facilities and development of test processes. Test results available via Duncan, et al., at this year's Data Workshop. | 3.3V, 5V, 12V | 1 |
| Skylake 6th Gen Core™ i3-6100 | Intel | 15-081 | Processor | 14nm Gen 6 CMOS and FinFET | H: (TAMU15Dec) CS | Test results available via Duncan, et al., at this year's Data Workshop. | 3.3V, 5V, 12V | 1 |
| Skylake 6th Gen Core™ i3-6100T | Intel | 15-081 | Processor | 14nm Gen 6 CMOS and FinFET | H: (TAMU16May) CS; P: (Scripps16May) CS | Testing to evaluate Proton facilities and development of test processes. Test results available via Duncan, et al., at this year's Data Workshop. | 3.3V, 5V, 12V | 2 |
| **Memory Device:** | | | | | | | | |
| MT29F128G08CBECBH6 | Micron | 201448, 14-088 | Flash Memory | 16 nm CMOS | H: (LBNL2015Aug; 15Dec) DC | [illegible] | 3.3V | 2 |
| **Si Power devices:** | | | | | | | | |
| BUY15CS23-01 Engineering samples | Infineon | [illegible] | MOSFET | Super-junction | H: (TAMU2015Nov21) JML | [illegible] | [illegible] | 5 |
| DG403 | Vishay | [illegible] | Analog Switch | CMOS | [illegible] | [illegible] | +/-15V | 6 |
| 2N6790 | International Rectifier | [illegible] | MOSFET | Power | [illegible] | [illegible] | 0 $V_{GS}$ | 2 |
| 2N6845 | International Rectifier | [illegible] | MOSFET | Power | [illegible] | [illegible] | 0 $V_{GS}$ | 2 |
| LM195 | National Semiconductor | [illegible] | Power Transistor | Bipolar | [illegible] | [illegible] | 35V | 4 |
| 1N5554 | Microsemi | [illegible] | Diode | Si | [illegible] | [illegible] | 500V | 62 |
| DSS17-06CR | IXYS | [illegible] | Diode | Si | [illegible] | [illegible] | 600 V | 5 |
| FST30100 | Microsemi | [illegible] | Diode | Si | [illegible] | [illegible] | 100 V | 3 |
| FYPF1545 | Fairchild Semiconductor | [illegible] | Diode | Si | [illegible] | [illegible] | 45 V | 3 |
| FYPF2045 | Fairchild Semiconductor | [illegible] | Diode | Si | [illegible] | [illegible] | 45 V | 3 |
| FYPF2006 | Fairchild Semiconductor | [illegible] | Diode | Si | [illegible] | [illegible] | 60 V | 3 |
| FYPF1010 | Fairchild Semiconductor | [illegible] | Diode | Si | [illegible] | [illegible] | 100 V | 3 |
| MBR2045 | Diodes, Inc. | [illegible] | Diode | Si | [illegible] | [illegible] | 45 V | 3 |
| MBR2060 | Diodes, Inc. | [illegible] | Diode | Si | [illegible] | [illegible] | 60 V | 3 |
| MBR20200 | Diodes, Inc. | [illegible] | Diode | Si | [illegible] | [illegible] | 200 V | 4 |
| MBR4050 | On Semiconductor | [illegible] | Diode | Si | [illegible] | [illegible] | 250 V | 5 |
| MBRF20100 | Diodes, Inc. | [illegible] | Diode | Si | [illegible] | [illegible] | 100 V | 4 |
| MBRF30100 | Diodes, Inc. | [illegible] | Diode | Si | [illegible] | [illegible] | 100 V | 4 |
| LXA03T600 | Power Integrations | [illegible] | Diode | Si | [illegible] | [illegible] | 600 V | 11 |
| LXA05T600 | Power Integrations | [illegible] | Diode | Si | [illegible] | [illegible] | 600 V | 11 |
| VS-APH3006-N3 | Vishay | [illegible] | Diode | Si | [illegible] | [illegible] | 600 V | 5 |
| SBL8L40 | Vishay | [illegible] | Diode | Si | [illegible] | [illegible] | 40 V | 3 |
| SBL1040 | Vishay | [illegible] | Diode | Si | [illegible] | [illegible] | 40 V | 3 |
| SBL1045 | Vishay | [illegible] | Diode | Si | [illegible] | [illegible] | 45 V | 3 |
| SBL3040 | Vishay | [illegible] | Diode | Si | [illegible] | [illegible] | 40 V | 3 |
| SBR20A300 | Diodes, Inc. | [illegible] | Diode | Si | [illegible] | [illegible] | 300 V | 5 |
| SBR30300 | Diodes, Inc. | [illegible] | Diode | Si | [illegible] | [illegible] | 300 V | 5 |
| **SiC Devices:** | | | | | | | | |
| CPM2-1200-0025B | CREE | [illegible] | MOSFET | SiC Gen 2 VDMOS | H: (LBNL2015Jul) JML | [illegible] | 0 $V_{GS}$ | 11 |
| CPM3-1200 Engineering samples | CREE | [illegible] | MOSFET | SiC Gen 3 VDMOS | [illegible] | [illegible] | 0 $V_{GS}$ | 6 |
| Test chip | GE | [illegible] | Diode | SiC IC | [illegible] | Contact PI for test results (data proprietary) | -100V | 2 |
| Engineering samples, various | GE | [illegible] | Diodes | SiC discrete | [illegible] | Contact PI for test results (data proprietary) | Various | 11 |
| Engineering samples | GE | 15-041 | MOSFET | SiC VDMOS | [illegible] | Contact PI for test results (data proprietary) | 0 $V_{GS}$ | 12 |
| STPSC10060 | STMicroelectronics | [illegible] | Diode | SiC | [illegible] | [illegible] | Various $V_R$ and angles | 4 |
| Test chip | GE | [illegible] | Frequency Divider | SiC IC | [illegible] | Contact PI for test results (data proprietary) | 12V-20V | 5 |
| Test chip | GE | [illegible] | Ring Oscillator | SiC IC | [illegible] | Contact PI for test results (data proprietary) | 5V-20V | 1 |
| Test chip | GE | [illegible] | Op Amp | SiC IC | [illegible] | Contact PI for test results (data proprietary) | 20V | 2 |
| IC test chip | Ozark IC | [illegible] | Op Amp | SiC IC | [illegible] | Contact PI for test results (data proprietary) | 15V | 3 |
| **Op Amps:** | | | | | | | | |
| OPA2107 | Texas Instruments | [illegible] | Op Amp | Difet | [illegible] | [illegible] | Various | 3 |
| AD8038 | Analog Devices | [illegible] | Op Amp | XFCB | [illegible] | [illegible] | +/-5V | 3 |
| LT2078 | Linear Technology | [illegible] | Op Amp | Bipolar | [illegible] | [illegible] | +/-15V | 3 |
| OP470 | Analog Devices | [illegible] | Op Amp | Bipolar | [illegible] | [illegible] | ±6V to ±15 V | 5 |
| OP200 | Analog Devices | [illegible] | Op Amp | Bipolar | [illegible] | [illegible] | 14.3 | 9 |
| OP400 | Analog Devices | [illegible] | Op Amp | Bipolar | [illegible] | [illegible] | 14.3 | 10 |
| **FPGA:** | | | | | | | | |
| RT4G150-CB1657MSX489 | Microsemi | [illegible] | FPGA | 65nm CMOS | [illegible] | [illegible] | 1.0, 2.5 and 3.3 V | 1 Rev B; 1 Rev C |
| XC7K325T Kintex7 | Xilinx | [illegible] | FPGA | 28nm CMOS | [illegible] | [illegible] | Varies w/data sheet | 3 |
| **Other Devices:** | | | | | | | | |
| HM628128 | Hitachi | 9249 | 1Mb SRAM | 0.8um CMOS | P: (MGH15Dec; TRIUMF15Oct) TW | [illegible] | 5V | 4 |
| Magnum Test Vehicle | IBM (now Global Foundries) | [illegible] | SRAM | 45 nm SOI CMOS | [illegible] | [illegible] | 0.6 to 1.2V | 1 |
| SPC56068 | NXP (Freescale) | [illegible] | Automotive Microcontroller | 90nm CMOS | [illegible] | [illegible] | 5V | 4 |
| AD5328 | Analog Devices | [illegible] | DAC | CMOS | [illegible] | [illegible] | 5V | 4 |
| MAX4180 | Maxim | [illegible] | LVDS | CMOS | [illegible] | [illegible] | 3.3-3.6V | 4 |
| ADV212 | Analog Devices | [illegible] | Video Codec | CMOS | [illegible] | [illegible] | 5V | 1 |

## Test Results and Discussion

As in our past workshop compendia of NASA Goddard Space Flight Center (GSFC) test results, each DUT has a detailed test report available online at http://radhome.gsfc.nasa.gov describing the test method, SEE conditions/parameters, test results, and graphs of data. This section contains summaries of testing performed on a selection of featured parts.

### *Analog Devices OP470 Operational Amplifier*

The OP470 is a high-performance monolithic quad operational amplifier with exceptionally low voltage noise. The OP470 features an input offset voltage below 0.4 mV and an offset drift under 2 µV/°C, guaranteed over the full military temperature range. Input bias is under 25 nA which reduces errors due to signal source resistance. The OP470's CMRR of over 110 dB and PSRR of less than 1.8 µV/V significantly reduce errors due to ground noise and power supply fluctuations. The OP470 is unity-gain stable with a gain-bandwidth product of 6 MHz and a slew rate of 2 V/µs.

The parts were prepared for testing by mechanically delidding each device. The parts were then soldered to small printed circuit boards (PCBs) that were designed specifically for this testing. Because this is a quad part, each op amp in the package was tested in a different configuration for analyzing transients and the destructive effects. In Fig. 1, the test circuits for one device (labeled A) were built to model/approximate the intended application. The configuration of device A was an application specific feedback design. This application-specific configuration also included an application-specific filter on the output. The second op amp (B) implemented the same application-specific feedback configuration, but did not include the output filter. This was used to determine the actual size of the transients generated by the op amp in the application-specific configuration. The third op amp (C), was a simple voltage follower with a gain of 1, but it also had the filter on the output. Finally, device D was also a unity gain voltage follower with no filter on the output.

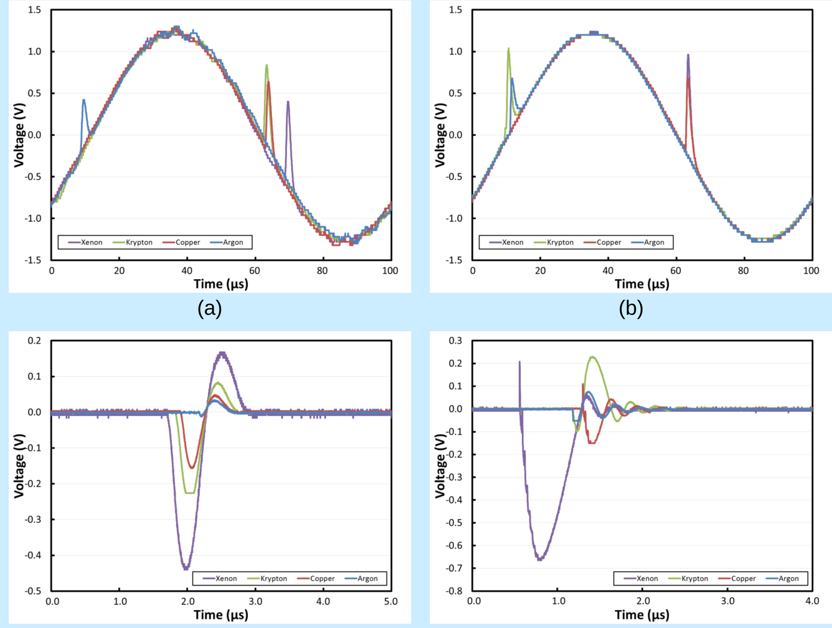


Fig. 1. Representative worst case transients are shown for (a) the application-specific circuit configuration with the application-specific output filter, (b) the application-specific circuit configuration with no output filter, (c) a unity gain voltage follower with the application-specific output filter, and (d) a unity gain voltage follower with no output filter. Transients generated from argon are shown in blue, copper is shown in red, krypton in green, and xenon in purple.

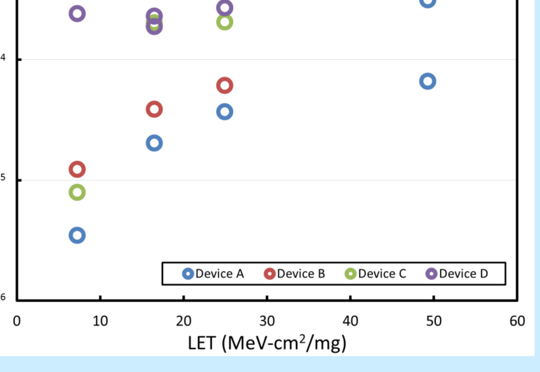


Fig. 2. The cross-section versus LET plot for the four different OP470 circuit configurations tested.

Because other work had indicated SEDR has been observed in other Analog Device's parts from the same product lines, it was necessary to determine the conditions under which SEDR occurred in this part. Destructive SEEs were observed during this testing; however, none were observed at the application supply voltage of ±6 V for any ion tested. After determining the part was not susceptible to destructive SEEs at the application voltage with any ion tested, the supply voltage was incrementally increased by ±1 V and irradiated until SEDR was observed, or the particle fluence reached $1\times10^7$ particles/cm². No destructive events were observed while irradiated at a 60° angle of incidence.

In addition to identifying the conditions under which the OP470 is susceptible to SEDR, we also captured transients for the four different circuit configurations. Figs. 10 a-d show the worst-case transients generated by the ions tested for each circuit configuration. Fig. 2 shows the SET cross section for each circuit configuration. The worst-case transients are approximately 1.5 µs wide and just under 1 V in amplitude.

### *Hitachi HM628128 1Mb SRAM*

The Hitachi HM628128LP-10 is a 1 Mbit (128k x 8) SRAM built on a 0.8µm CMOS process. The devices tested have a date code of 9249. Both ground-test and in-flight data have previously been published on this part in It was selected to be the test vehicle for a series of proton experiments intended to directly compare different proton facilities, both scientific and medical.

The HM628128LP-10 was tested at TRIUMF in Vancouver, BC, Canada, and exposed to 480 MeV and 105 MeV proton beams. Each run was to a total fluence of $1\times10^{10}$ protons over approximately 100 seconds. That fluence produces approximately 1000 byte-errors in this device, representing about 1% of the memory array. Prior to each run, the part was power-cycled and programmed with a repeating data pattern. The part was irradiated under nominal bias, and then read to determine the number of addresses in error. This process was repeated several times for each data pattern at each proton energy. A second test was performed at Massachusetts General Hospital's Proton Therapy Center (MGH). The devices were configured and tested in the same manner as before, but exposed to a 200 MeV proton beam.

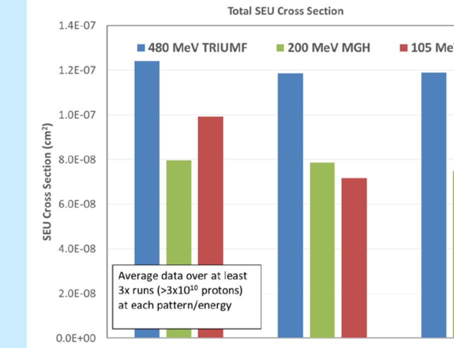


Fig. 3. Total SEU cross section measured at TRIUMF, with data broken down by memory pattern and beam energy.

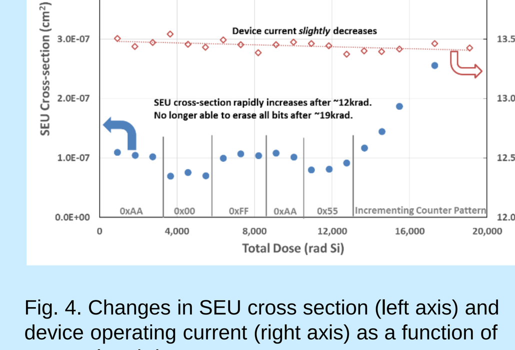


Fig. 4. Changes in SEU cross section (left axis) and device operating current (right axis) as a function of accumulated dose.

SEU cross-sectional data were obtained from both tests and plotted [Fig. 3]. Additionally, total ionizing dose was logged for each run, and cross-sectional data re-plotted as a function of cumulative dose [Fig. 4] to verify the total dose limitations of this device. SEU rates began to increase rapidly after approximately 14 krad (Si) of proton irradiation regardless of energy tested.

The data from TRIUMF, MGH, and previously published data on this part will be utilized as a baseline for comparing additional proton test facilities across a variety of proton energies. It is expected that further data will be needed to shed light on the apparent inconsistencies in proton energy vs upset rate suggested by the initial results of Fig. 4.

### *Intel Core™ i3-5005u "Broadwell" Mobile Processor; Core™ i5-6600K, i3-6100, i3-6100T "Skylake" Desktop Processor*

Commercially available state-of-the-art (SOTA) processor technologies remain an active topic of our interest. Our efforts remain focused on products offered by Intel that are based on their 14nm "Tri-Gate" design process: The Core™ i3-5005u "Broadwell" family mobile processor and a trio of "Skylake" family desktop parts: the Core™ i5-6600K, i3-6100, and i3-6100T. While testing these devices remains, in and of itself, a fascinating challenge, the real highlight of our activity was the opportunity to leverage inter- and intra-agency cooperative efforts to achieve mutual end goals

At last year's NSREC Data Workshop, we presented TID test results on the i3-5005u part, continuing a long-standing working relationship with Naval Surface Warfare Center (NSWC) Crane. Within this study, we detailed an in-situ test designed to "stress" the part with an intensive workload after periodic amounts of TID exposure. Due to time constraints, the DUT could only be tested up to 4 Mrad (Si), but no hard failures occurred.

Prior to our TID testing at NSWC Crane, an invitation was extended by the NEPP Program to participate in their evaluation of North American proton facilities. In exchange for the opportunity to collect interesting data at various sites, our challenge was to familiarize ourselves with the process of operating unfamiliar beam lines and recording observations detailing our perceived level of difficulty with respect to experiment setup

From May of 2015 to May of 2016, our "Broadwell" test setup would travel to Scripps, HUPTI, TRIUMF, and MGH for proton testing. Fig. 5 shows the Broadwell test set-up at Scripps and Fig. 6 shows the gantry room at HUPTI. In-between proton facility visits, we also conducted heavy ion tests with Ne and Ar at TAMU.

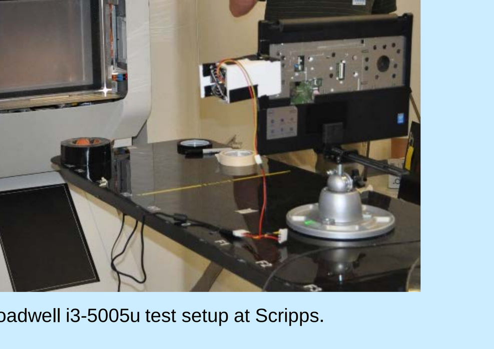

Fig. 5. Broadwell i3-5005u test setup at Scripps.

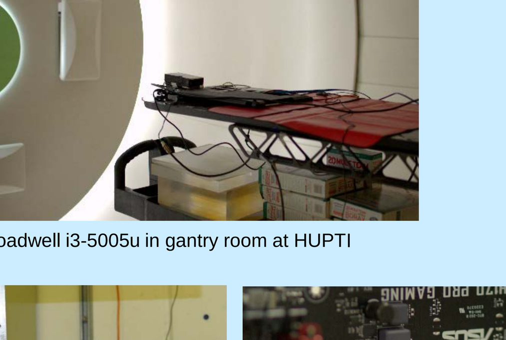

Fig. 6. Broadwell i3-5005u in gantry room at HUPTI

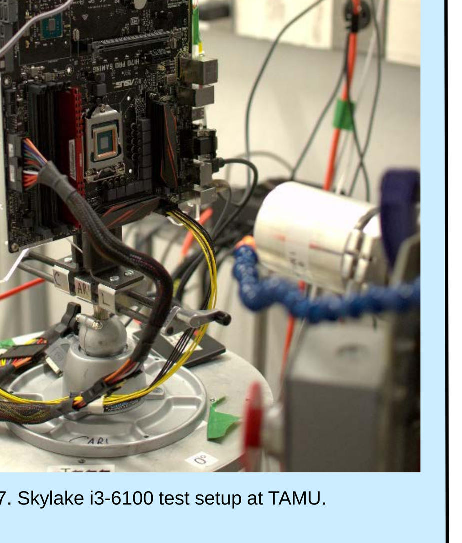

Fig. 7. Skylake i3-6100 test setup at TAMU.

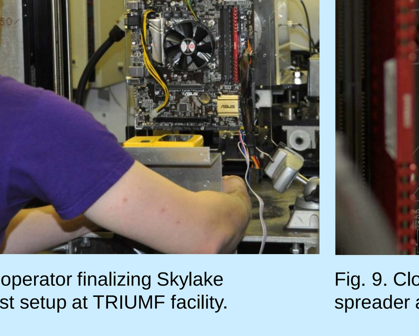

Fig. 8. Test operator finalizing Skylake i5-6600K test setup at TRIUMF facility.

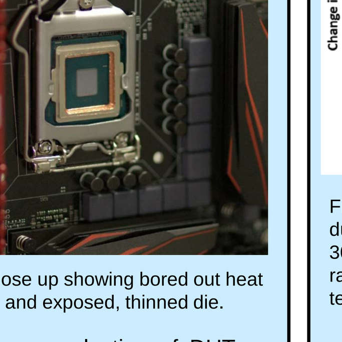

Fig. 9. Close up showing bored out heat spreader and exposed, thinned die.

With regard to our "Skylake" family processors, our selection of DUTs reflected market availability at the time of the facility visit: the 91W TDP Core™ i5-6600K (11/2015 TRIUMF), Fig. 8 shows the operator finalizing the test setup at TRIUMF, the 51W TDP Core™ i3-6100 (12/2015 TAMU), and the 35W TDP Core™ i3-6100T (5/2016 TAMU & SCRIPPS). The goal was to be ready to acquire data points as circumstances and test trips warranted. Fig. 7 shows the Skylake set-up for TAMU and Fig. 9 shows a close up of the exposed die.

Data collected has been combined with NSWC independently collected test results. See A. R. Duncan, et al., for complete details of this work and test setup.

As we continue the proton facility study combined with our processors / SOTA technology evaluation, we hope to yield more information on how these parts behave under irradiation, and further refine how best to conduct tests on these complex devices. At the same time, with these parts being relatively inexpensive, they can continue to serve as a simple means to understand the inner workings of various test facilities and provide an infinite source of entertainment to the investigators.

### *Cree CPM2-1200-0025B SiC VDMOS*

Heavy-ion SEE tests were conducted at the Lawrence Berkeley National Laboratory (LBNL) in vacuum with 10 MeV/u xenon or argon. The bare die were assembled in TO-3 headers without lids, and a controlled 1-mil parylene-C coating was then deposited to prevent the bond wires from arcing under high voltage. Beam energy at the surface of the die after passing through the coating was determined using the SRIM code to be 966 MeV for xenon, with an LET in SiC of 65 MeV-cm²/mg and a penetration range of 45 mm; for argon, energy = 361 MeV, LET = 11 MeV-cm²/mg, and range = 77 mm. Prior to and after each irradiation, the gate-source leakage current ($I_{GSS}$) and drain-source leakage current ($I_{DSS}$) and/or the breakdown voltage were measured. During irradiation, $V_{GS}$ was held at 0 V, a positive $V_{DS}$ was applied, and the gate and drain currents were continuously measured and recorded via Keithley 2635A or 2400, and 2657A SMUs.

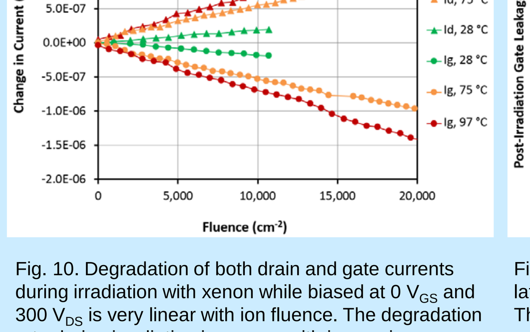


Fig. 10. Degradation of both drain and gate currents during irradiation with xenon while biased at 0 $V_{GS}$ and 300 $V_{DS}$ is very linear with ion fluence. The degradation rate during irradiation increases with increasing case temperature.

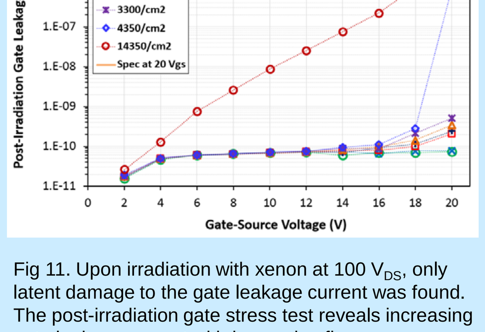


Fig 11. Upon irradiation with xenon at 100 $V_{DS}$, only latent damage to the gate leakage current was found. The post-irradiation gate stress test reveals increasing gate leakage current with increasing fluence.

Immediate catastrophic failure of the device occurred upon xenon beam exposure at 600 $V_{DS}$. At lower voltage, permanent degradation of the drain and/or gate leakage current occurred linearly as a function of fluence. The slope of this degradation increased with increasing temperature, as can be seen in Fig. 10 where the change in leakage current during the beam run as a function of fluence is shown for a single part irradiated at 300 V with xenon at 28 °C, 75 °C, and 97 °C case temperature. In silicon power MOSFETs, SEB susceptibility during radiation testing is often reduced by elevated temperature due to the decreased charge mobility. SEB in silicon power MOSFETs typically involves the turn-on of the parasitic bipolar junction transistor. The behavior of silicon carbide power MOSFETs differs: in addition to immediate catastrophic failure, there is a voltage range at which permanent substantial degradation of leakage current occurs that worsens with increasing temperature. It is most likely that the mechanisms in SiC MOSFETs are direct and do not involve the parasitic bipolar transistor.

In addition to burnout in the SiC material, the MOSFETs are susceptible to latent damage in the gate oxide. As shown in Fig. 11 for the CPM2-1200-0025B irradiated under 100-V drain-source bias with xenon, this degradation is fluence-dependent, such that no single ion causes the part to go out of specification under these conditions. Irradiation with the much lighter ion, argon, at 100 $V_{DS}$ up to a fluence of $5\times10^5$ cm$^{-2}$ resulted in no measurable change in $I_{GSS}$.

## Summary

We have presented current data from SEE testing on a variety of mainly commercial devices. It is the authors' recommendation that these data be used with caution. We also highly recommend that lot testing be performed on any suspect or commercial device.

## Acknowledgment


This work was supported in part by the NASA Electronic Parts and Packaging Program (NEPP), NASA Space Technology Mission Directorate Game Changing Technology Division, and NASA Flight Projects.

The authors gratefully acknowledge members of the Radiation Effects and Analysis Group who contributed to the test results presented here: Raymond L. Ladbury, Hak Kim, Anthony M. Phan, Daniel P. Violette, Donna J. Cochran, Donald K. Hawkins, James D. Forney, Christina M. Seidleck, Martin A. Carts, Marco A. Figueiredo, Yevgeniy Gerashchenko, Robert A. Gigliuto, and Stephen R. Cox. Also thanks to Yusif A. Nurizade, formerly with NASA GSFC, Power Systems Branch.

Thanks to the High Temperature Boost Power Processing Unit Project, funded by the Game Changing Technology Division, NASA Space Technology Mission Directorate for its support. We extend thanks to the NEPP Program for providing the invaluable opportunity to include proton test experiments in conjunction with its ongoing evaluation of proton facilities for radiation effects testing.

Special thanks go to Stephen P. Buchner and Dale McMorrow, Naval Research Laboratory for their excellent support of the laser testing



To be presented by Martha O'Bryan at the 2016 Electrical and Electronics Engineers (IEEE) Nuclear and Space Radiation Effects Conference (NSREC), Portland, Oregon, July 11-15, 2016.